



HAL
open science

Effect of heat treatment on *Pinus pinaster* rosin: A study of physico chemical changes and influence on the quality of rosin linseed oil varnish

Manon Francès, Yanis Gardere, E. Duret, Léo Leroyer, Thomas Cabaret, M. Rubini, Arsène Bikoro Bi Athomo, Bertrand Charrier

► To cite this version:

Manon Francès, Yanis Gardere, E. Duret, Léo Leroyer, Thomas Cabaret, et al.. Effect of heat treatment on *Pinus pinaster* rosin: A study of physico chemical changes and influence on the quality of rosin linseed oil varnish. *Industrial Crops and Products*, 2020, 155, pp.112789 -. 10.1016/j.indcrop.2020.112789 . hal-03492057

HAL Id: hal-03492057

<https://hal.science/hal-03492057>

Submitted on 7 Jan 2022

HAL is a multi-disciplinary open access archive for the deposit and dissemination of scientific research documents, whether they are published or not. The documents may come from teaching and research institutions in France or abroad, or from public or private research centers.

L'archive ouverte pluridisciplinaire **HAL**, est destinée au dépôt et à la diffusion de documents scientifiques de niveau recherche, publiés ou non, émanant des établissements d'enseignement et de recherche français ou étrangers, des laboratoires publics ou privés.

1 Effect of heat treatment on Pinus pinaster rosin: a study of physico chemical changes and
2 influence on the quality of rosin linseed oil varnish

3 Frances, M. ^{a*}, Gardere, Y. ^a, Duret, E. ^a, Leroyer, L. ^a, Cabaret, T. ^a, Rubini, M. ^a, Bikoro Bi
4 Athomo, A. ^a, Charrier, B^a

5 ^aCNRS/ Univ Pau & Pays Adour, Institut des Sciences Analytiques et de Physico-Chimie pour
6 l'Environnement et les Matériaux, Xylomat, UMR5254, 40004, Mont de Marsan, France

7 Corresponding author: manon.mg.frances@gmail.com

8 Abstract:

9 The aim of this study was to get a better understanding of the formulation aspect of a new
10 linseed oil – rosin varnish inspired by the antique violin coating, using heat-treated and non-treated
11 rosin. To do so, the heat treatment effect on rosin was studied on both its thermal properties and some
12 of the varnish properties. The rosin without heat treatment was assigned as the reference. The
13 temperature treatments were: 180 °C, 200 °C and 250 °C. The thermal properties were studied using
14 TMA, DSC, ATG and HPLC. A change due to heat treatment was observed, especially on the
15 softening point and the glass transition, which increase with the temperature. Chemical changes were
16 observed, with the apparition of dehydrogenated and oxidised forms of abietane-based acid, which are
17 not present in the reference rosin. As expected, the amount of turpentine decreases with the heat
18 treatment. The varnish properties are also impacted, with a decrease of brightness and solvent
19 resistance with the temperature. A PCA was made in order to have a statistical analysis of the results.
20 Through this, a clear separation of the four groups was graphically observed, with different
21 representative variables. The variables' influence on each other was also clearly identified, as well as
22 the impact of the chemical changes on thermal and varnish properties.

23 Keywords: rosin, formulation, vegetable oil, maritime pine, varnish, heat treatment

24

25 1. Introduction

26 *Pinus pinaster*, also known as Maritime pine is present in vast areas of Italy, France, Portugal,
27 Spain and North of Africa. The largest monospecific woodland in south-western Europe extends over
28 the Landes de Gascogne: a 1.5 million hectare maritime pine forest (Rosa et al., 2018). The maritime
29 pine is cultivated for its timber (Pinto et al., 2005; Riesco Muñoz et al., 2014). Historically, it was used
30 to harvest resin (Soliño et al., 2018). Maritime pine contains more resin ducts than other conifers (Wu
31 and Hu, 1997), connected by anastomoses (Rodríguez-García et al., 2014). Conifers in the pine family
32 also have the ability to form new resin ducts following biotic and abiotic attacks (Krokene, 2015). The
33 resin is produced in epithelial cells, and accumulated in resin ducts (Wu and Hu, 1997). The harvest is
34 made by pine tapping, a process based on the defence system of the tree, which secretes resin as a
35 defensive response to external factors (Rodríguez-García et al., 2016). This defence mechanism can
36 come into play as a response to phytopathogenes (Franceschi et al., 2005), abiotic stress (Blanche et
37 al., 1992), chemical stimuli (Moreira et al., 2009), or, in our case, mechanical wounding (Cheniclet,
38 1987). After distillation, resin is separated into a volatile fraction, the turpentine (30 %), and a solid
39 residue, the rosin (70 %) (Hawley and Palmer, 1912). The rosin is a brittle, glassy solid, with a yellow-
40 brown colour (Coppen and Hone, 1995).

41 Rosin composition has been investigated for several years. It contains 90 % of diterpenic
42 acids, and its empirical formula is $C_{20}H_{30}O_2$. The composition may vary depending on its source,
43 species and geographical area. There are two main types of acids in the rosin, pimaric-like and abietic-
44 like. The abietic-like includes: abietic, neoabietic, palustric, and dehydroabietic acid. The pimaric-like
45 includes: dextropimaric and isodextropimaric (Baldwin et al., 1958; Joye and Lawrence, 1967). The
46 softening point has been determined with thermomechanical analysis (TMA) developed by Cabaret et
47 al., which could be more precise than the ASTM E28-14 standard, and is between 25 °C to 70 °C
48 (Cabaret et al., 2018). According to Gaillard et al. (2011), rosin does not have a precise glass transition
49 temperature, but a wide temperature range before reaching a liquid state. The thermal decomposition
50 of rosin occurs in a temperature range from 190 °C to 310 °C (Narayanan et al., 2017). Rosin has
51 many applications such as adhesives (Wang et al., 2018), antibacterial polymer (Kanerva et al., 2019)
52 or packaging (Narayanan et al., 2017). It has been widely used from the 16th through to the early 19th

53 century for varnish by violin makers (Echard and Malecki, 2014). There are numerous studies about
54 those varnishes (Chen, 1992; Echard et al., 2010; Invernizzi et al., 2016), which highlight a blend of
55 siccative oil, rosin and siccative additives (lead, aluminium, iron).

56 Previous studies have observed the proportion, preparation and molecular composition of
57 these historical varnishes (Tirat et al., 2017, 2016), revealing the interaction between the triglycerides
58 from the linseed oil and the diterpenic acids ; they most probably react together to form hybrid species,
59 oligomeric diterpenes and/or hybrid glyceride-diterpene species. It is likely that the heat treatment is
60 what causes the formation of acid species. The heat treatment of linseed oil has previously been
61 studied (Byrdwell and Neff, 1999): increasing the temperature results in a higher degree of oxidation
62 and increases the average molecular weight (Berg, 2002). The heat treatment has also been studied for
63 the rosin. The abietic based acids undergo isomerization, due to their two conjugated double bonds,
64 decomposition, dehydrogenation (Chen, 1992; Loeblich et al., 1955) and auto-oxidative
65 polymerization during the heating (Artaki et al., 1992). Those modifications lead to the formation of
66 compounds such as 15-hydroxo-dehydroabietic acid, 7-oxo-15-hydroxy-dehydroabietic acid and 7-
67 oxo-dehydroabietic acid (Cabaret et al., 2019; Scalarone et al., 2002).

68 The objective of this study is to characterize the rosin before and after high-temperature heat
69 treatment (180 °C, 200 °C and 250 °C) with differential scanning calorimetry (DSC),
70 thermogravimetric analysis (TGA), TMA and high-performance liquid chromatography (HPLC), and
71 to qualify the consequences of those treatments in linseed oil – rosin varnishes. A principal component
72 analysis (PCA) was conducted, in order to correlate the rosin results with the varnishes. PCA is a
73 multivariate technique that aims to reduce the number of dimensions in a dataset (Wold et al., 1987).
74 The purpose is to obtain information in order to create a new varnish, inspired by the antique violin
75 coating and using a local resource for our research team localisation, the rosin.

76 2. Materials and methods

77 2.1 Raw materials

78 The rosin came from a batch obtained after distillation of one resin mixture from various
79 maritime pine trees from the Landes forest, extracted with the Biogemme© eco-process. It was
80 furnished by Holiste, Biscarosse, France. [This rosin is used raw as a reference](#). The distillation, in
81 order to obtain pure rosin, was made by Biolandes, Le Sen, France, at low temperature and low
82 pressure; details of this process are confidential. The raw linseed oil, [first pressing and 100 % from](#)
83 [linseed](#), was provided by Onyx, Roche-lez-Beaupré, France. Ôkhra company based in Roussillon,
84 France, supplied the umber powder, [containing manganese dioxide and iron oxide, known as driers for](#)
85 [linseed oil. Indeed they promote peroxide decomposition and reduce the induction time \(de Viguerie et](#)
86 [al., 2016\)](#).

87 2.2 Heat treatment

88 The reference rosin (Holiste, Biscarosse, France) was used without heat treatment. The rosin
89 degradation temperature range starts at 200 °C and ends around 300 °C (Artaki et al., 1992), therefore
90 the heat treatment temperatures were chosen [within that range](#). All the rosin samples were heated for
91 30 minutes [with a stirring hot plate at 180 °C, 200 °C and 250 °C, corresponding respectively to the](#)
92 [linseed oil temperature in the varnishes preparation, the onset temperature of rosin degradation and](#)
93 [temperature where degradation occurs. It was decided to not test the 300 °C temperature, which is too](#)
94 [close to the self-ignition temperature of the rosin, 390 °C \(Carson and Mumford, 2002\)](#).

95 2.3 Varnishes preparation

96 All varnishes were [prepared](#) using the same protocol, to [ensure](#) reproducibility of the different
97 steps. Linseed oil was first heated in a glass beaker at 180 °C [for 220 minutes](#) according to the recipe
98 of the [instrument maker](#) Nicolas Gilles (Gilles, 2019). UMBER powder was added as a siccative during
99 the heating, [at 0,2 % weight of the total varnish mass](#). After the heating time, the mixture was brought
100 to room temperature. The rosin was grinded in a mortar before sifting at 800 µm, and then added to the
101 mixture with a 20/80 [\(rosin/linseed oil\)](#) w/w ratio at room temperature. The mixture was heated at 180
102 °C [for a duration of 90 minutes](#) under constant stirring. At the end, heating was cut and the varnish

103 was allowed to cool down to room temperature. The varnish was poured into a UV-protected vial and
104 kept at room temperature.

105 2.4 Varnish application

106 Each varnish was applied with a brush on three maritime pine panels, and UV polymerized.
107 The panel dimensions were 150 x 74 x 18 mm. The UV lamp had a wavelength of 340 nm, and an
108 irradiance of 1,55W/m². Each layer of coating required 6 hours of UV exposition in order to
109 polymerize. Three layers were needed, in order to obtain a satisfying homogeneity. The three layers
110 gave a final film thickness between 150 and 200 μm.

111 2.5 Differential scanning calorimetry (DSC) analysis

112 Measurements were carried out on a DSC (TA Instruments, Q20) equipped with a rapid
113 cooling system. Individual samples of heat-treated rosin and the reference were weighed (~5 mg) in
114 standard aluminium pans (TA Instruments) and data acquisitions were carried out using the Universal
115 Analysis 2000 program (TA Instruments). Samples were first dried using an isotherm at 105 °C for 1
116 minute followed by a cooling step at the rate of 10 °C/min. Then, samples were scanned under air
117 atmosphere between 20 °C and 110 °C at a heating rate of 10 °C/min. All experiments were repeated
118 three times. The maximum temperature of 110 °C was chosen from the literature (Coppen and Hone,
119 1995; Gaillard et al., 2011). The experiment has been tested in a range from 5 °C to 200 °C, but no
120 transition has been observed, as shown in Fig. 1.

121 *Figure 1 : DSC thermogram of reference rosin in a range from 5 °C to 200 °C*

122 2.6 Thermogravimetric analysis (TGA)

123 Thermal decomposition analysis of heat-treated rosin and the reference sample was performed
124 by TGA (TA Instruments, Q20). Under flow of air at 60 ml/min, samples (10.0 ± 2.0 mg) of rosin
125 were heated under temperature conditions ranging from 30 °C to 600 °C at a heating rate of 10
126 °C/min. An isotherm was kept for 20 min at 150 °C, in order to determine the turpentine amount in the
127 rosin. All experiments were repeated three times.

128 2.7 Softening point measurement

129 According to ATSM E28-14, American standard for measuring this softening point, rosin is
130 liquefied by heating before being cooled and solidified in a ring. This ring is placed in a beaker filled
131 with water, then a ball is placed on the solidified rosin, and the system is heated, until it liquefies. This
132 causes the ball to fall through the rosin. The softening temperature is noted when the ball hits the
133 bottom of the beaker. However, this technique involves a first heat treatment of the rosin, to liquefy it
134 before measuring its softening point. Heat treatment has an influence on its softening properties. This
135 is why we opted to use a technique enhanced by Cabaret et al. (2018), where the softening point of the
136 rosin was measured using TMA. Measurements were carried out using a TMA (Mettler Toledo,
137 SDTA840) and a standard probe. Samples with a thickness of 5 mm of heat-treated rosin and the
138 reference were prepared by breaking small pieces of hard rosin, without heating, and placed between
139 the probe and the support. A constant force of 0.02 N was applied and the sample was scanned at a
140 heating rate of 2 °C/min between 25 °C and 200 °C above the sample softening point. Thickness
141 measurements were performed each second with the shifting of TMA probe according to the thermal
142 gradient. Thickness was measured each second and softening point temperature was determined at 100
143 µm, after the inflection point where the sample's height begins to quickly decrease due to the
144 penetration of the probe. All experiments were repeated three times.

145 2.8 High-performance liquid chromatography (HPLC) analysis

146 All samples (1% w/v in methanol) were analysed by RP-HPLC-DAD (Ultimate 3000, Thermo
147 Scientific) equipped with an Acclaim Polar Advantage II (3 mm x 150 mm, 3 µm, Thermo Scientific),
148 in methanol(A)/water(B) multi-gradient mode at 1 ml/min (injection volume 10 µL). The gradient
149 elution program was set as follows: 0-2 min.: (60%) A, 2-17 min.: (60-80%) A, 17-24 min. (80%) A,
150 24-35 min. (80-100%) A, 35-44 min. (100%) A. Then, the elution gradient was linearly ramped down
151 to 60% A for 2 min. Finally, this gradient was maintained for 9 min in order to find the initial
152 conditions of the column for the next injection. All experiments were repeated fifteen times.

153 2.9 Mechanical properties

154 2.9.1 Thickness

155 The thickness was measured in μm , using an ultrasonic coating thickness-measuring device
156 (PosiTector 200). Three measurements were made on each panel.

157 2.9.2 Colour

158 The measurements were made using a spectrophotometer (X-rite, Ci62), according to the NF
159 EN ISO 18314 standard. The colour was expressed using the CIEL*a*b* colour space, which
160 expresses colour as three numerical values: L* for the lightness, a* for the green–red chromatic
161 coordinate and b* for the blue–yellow chromatic coordinate. Three measurements were made on each
162 panel.

163 2.9.3 Brightness

164 The brightness was measured at an angle of 60° , using a glossmeter (Byk-Gardner, micro-tri-
165 gloss), according to the NF EN ISO 2813 standard. Three measurements were made on each panel.

166 2.9.4 Adhesion

167 The measurements were carried out using a crosscut adhesion test kit (TQC), according to the
168 NF EN ISO 2409 standard. A grip with cutter was used to make two series of parallel cuts cross-
169 angled with each other to obtain a pattern of 25 similar squares. The ruled area was evaluated after a
170 short treatment with adhesive tape, using a table chart from 0 to 5, 0 being the highest score (no
171 varnish removed from the substrate). Three measurements were made on each panel.

172 2.9.5 Solvent resistance

173 The solvent resistance was measured using a sodium hydroxide solution at 5 % mass fraction,
174 according to the ISO 2812-4 standard. The panels were placed at a 30° angle from horizontal, and the
175 solvent drops were applied every one or two seconds for 10 min through a burette. After the solvent
176 application, the blistering was visually evaluated. Not according to the standard, it was decided to
177 evaluate the colour and the brightness after the solvent application. Three measurement were made on
178 each panel.

179 2.10 Principal Component Analysis (PCA) procedure

180 PCA helps to explain a data set with fewer linear combinations of the original variables, called
181 principal components (PCs). The procedure is to find PCs that explain most of the variation in the
182 data. Extracted PCs are ordered in an increasing explained variance. PCs represent the linear
183 combination of all variables included in the study. PCs are also called loadings because each original
184 variable is associated to weight (coefficient). All PCs are associated with the contribution of samples;
185 a score denotes this contribution.

186 A 12 x 17 matrix (where 12 is the number of samples, and 17 is the number of variables) was
187 used for the calculation. PCA on mean-scaled data was performed in R 3.6.0 (using RStudio Desktop
188 1.2.1335 interface) with FactoMineR (Lê et al., 2008) and Factoextra (Kassambara, 2017) packages.
189 The results of the analysis are presented in terms of Biplot.

190 3. Results and discussion

191 3.1 Thermal properties

192 3.1.1 Thermal degradation

193 The TGA thermograms of the reference and the heat-treated rosin are presented in Fig. 2. [The](#)
194 [raw rosin is used as a reference.](#)

195 *Figure 2 : TGA thermograms of rosin according to their heat treatment*

196 The weight loss at 150 °C corresponds to the turpentine fraction of the rosin, which will be
197 discussed in the chemical composition part of this paper. For all the samples, the main degradation
198 occurs at about 200 °C and finishes at about 350 °C, [as observed by Kanerva et al. \(2019\).](#) The final
199 mass loss observed with TGA for the [reference](#) and the heat-treated rosins are presented in Fig. 3.

200 *Figure 3: Comparison of the final mass loss of rosin according to their heat treatment. The standard*
201 *deviation is calculated over 3 samples.*

202 This final mass loss appears to be relatively unaffected by the heat treatment, which is
203 confirmed by the student test.

204 This observation is consistent with the mechanisms proposed by Artaki et al., (1992) at 250
205 °C. In this study, this degradation observed at 250 °C corresponds to isomerization followed by
206 dimerization, forming a mixture of dimeric diterpenes. In addition, under air, a mechanism of self-
207 oxidation occurs through the formation of hydroperoxides, forming glycols, ketones and esters of
208 varying molecular weights (Artaki et al., 1992). Finally, the degradation observed at 250 °C
209 corresponds to the formation of new compounds through oxidation and isomerization, and not to the
210 formation of small volatile molecules leading to a loss of mass. In our case the degradation caused by
211 heat treatment (below 250 °C) does not lead to a different final mass loss, which is consistent with the
212 study by Artaki et al., (1992). There is no relevant difference in the organic compounds/ashes ratio
213 between the samples. The chemical composition will be checked with HPLC analysis.

214 3.1.2 Softening point measurement

215 The softening point is determined at 100 µm after the bending point, which is when the sample
216 thickness begins to shrink, due to the penetration of the TMA probe. Fig. 4 describes the thickness
217 variation of all rosins, according to their heat treatment (raw for the reference, 180 °C, 200 °C and 250
218 °C).

219 *Figure 4: Thickness variation against temperature for rosins according to their heat treatment*

220 The softening point temperatures, measured with TMA, of all rosins are shown in Fig.5.

221 *Figure 5: Comparison of the rosin softening point temperatures according to their heat treatment. The*
222 *standard deviation is calculated over 3 samples.*

223

224 The values are different to the values obtained by Coppen and Hone, using ASTM E28-14,
225 which give softening points rather around 70 – 80 °C (Coppen and Hone, 1995). In addition, it appears
226 that the softening temperature of the rosin increases with the treatment temperature, which is
227 confirmed by the student test.

228 Reference rosin (raw) has a significantly different softening point from thermally treated
229 rosins. Heat treatment therefore increases the softening temperature of the rosin. This is consistent

230 with the observations of Cabaret et al. (2018), who showed that the rosin heated at 120 °C for 12 hours
231 might have a softening point 18 °C higher than that of the reference. This may be due to evaporation
232 of residual turpentine and/or chemical transformation of thermally treated rosin (with oxidation,
233 dehydrogenation and isomerization reactions). This will be checked with the turpentine amount
234 analysis by TGA and the composition analysis by HPLC.

235 3.1.3 Phase transition temperature measurement

236 Fig. 6 shows the DSC curves obtained for the reference and the heat treated rosin. A phase
237 transition temperature is clearly observed between 45 and 60 °C according to their heat treatment.

238 *Figure 6: DSC curves obtained for rosins according to their heat treatment*

239 This transition had not previously been observed by Gaillard et al. (2011), because, according
240 to this study, the rosin is completely amorphous. In our experiments, the rosin is distilled and purified
241 with the patented process at low temperature and low pressure, which are not the same conditions as
242 Gaillard et al. (2011) experiments and can lead to a more homogeneous product. Its physico-chemical
243 properties can be different. Indeed, this transition has been observed by Cabaret et al. (2018) on
244 industrial rosin and acetone extracted rosin. This study shows that the transition phase temperature,
245 comparable to glass transition according to Schilling (1989), can be observed when the rosin is
246 homogeneous.

247 The phase transition temperature of all rosins, reference and heat-treated, measured with DSC,
248 are presented in Fig. 7.

249 *Figure 7: Comparison of the rosin glass transition temperature according to their heat treatment. The
250 standard deviation is calculated over 3 samples.*

251 According to the student test, all the phase transition temperatures, which can be compared to
252 the glass transition temperature, are significantly different, except between the 200 °C and 250 °C
253 heat-treated rosins. This confirms the previous results obtained on the softening point of the rosin: the
254 heat treatment induces a softening, and thus a phase transition, at higher temperatures than for the

255 reference. The following analysis of residual turpentine content and chemical composition may be
256 used to validate the hypothesis of evaporation of residual turpentine, and/or a chemical transformation
257 of the thermally treated rosin (always according to oxidation, dehydrogenation and isomerization
258 mechanisms) leading to this phase transition to higher temperatures.

259 3.2 Chemical composition

260 3.2.1 Residual turpentine amount

261 The residual level of turpentine in the rosin was measured with TGA, where an isotherm at
262 150 °C was performed for 20 minutes to evaporate residual turpentine. As seen in Fig. 1, the weight
263 loss at 150 °C corresponds to the residual turpentine. The turpentine starts boiling from 150 °C, due to
264 the boiling temperature of its major compounds: α -pinene between 154 °C and 159 °C and β -pinene
265 (between 156 °C and 166 °C) (Hawkins and Armstrong, 1954). Fig. 8 shows the amount of turpentine
266 in the rosin according to their heat treatment. Overall, all the rosin have a low turpentine amount,
267 under 3 %, and even lower with the increased heat treatment. However, these results show that the
268 turpentine loss is not linear, the amount of turpentine being close between the heat-treated rosin.

269 *Figure 8: Comparison of the turpentine amount in rosin according to their heat treatment. The*
270 *standard deviation is calculated over 3 samples.*

271 These results have been submitted to a student test, in order to evaluate the differences
272 between them. According to this test, the raw rosin is significantly different from the heat-treated
273 ones; the 180 °C heat-treated rosin is significantly different from the 250 °C heat-treated one, while
274 the others heat-treated are not significantly different. Obviously, the residual turpentine is much lower
275 after treatment at 180 °C and above, as its boiling point is between 150 °C and 180 °C. The small
276 difference between 180, 200 and 250 °C can be explained by the difficulty to remove all the turpentine
277 in the rosin (Cbaret et al., 2019).

278 The results obtained confirm the hypothesis of a lower level of turpentine for higher softening
279 and phase transition temperatures. Glass transition temperature and softening point increase with heat
280 treatment, and do not vary much for high processing temperatures, 200 °C and 250 °C. The opposite

281 trend is observed with residual turpentine: it decreases with heat treatment, and does not vary much for
282 high treatment temperatures. However, the residual turpentine amount of the 180 °C treated rosin is
283 very close to the ones of the 200 and 250 °C treated rosins, whereas the phase transition temperatures
284 of the 180 °C rosin is significantly different from the ones of the 200 and 250 °C treated rosins. Thus,
285 the differences observed between the phase transition temperatures cannot be explained only by the
286 evaporation of the turpentine. Indeed, heat treatment can also be affected by the chemical composition
287 (Cabaret et al., 2018).

288 3.2.2 Abietane-based acids composition

289 All the rosin samples were analysed by HPLC, the raw rosin used as a reference, and the heat-
290 treated ones (at 180 °C, 200 °C and 250 °C). The chromatograms are presented in Fig. 9.

291 *Figure 9: HPLC chromatograms at 254 nm wavelength absorption of rosins according to their heat*
292 *treatment. (1) 7-oxo-dehydroabietic acid (7-oxo-DHA), (2) Abietane-based dehydroabietic acid*
293 *(DHABA), (3) Dehydroabietic acid (DHA), (4) Palustric acid, (5) Abietic acid, (6) Neoabietic acid*

294 Previous work by Cabaret et al., (2019) on rosin analysis by HPLC-MS, coupled with a
295 comparison of UV profiles of compounds based on results from Kersten et al. (2007), allows the
296 identification of the abietane-based acids and derivatives. Dehydroabietic acid (DHA) peak was
297 assigned based on the study by Kersten et al. (2007). A second abietane-based dehydrogenic acid
298 (DHABA) was also detected but could not be identified precisely. According to Cabaret et al. (2019)
299 and (Pastorova et al., 1997), 7-oxo-dehydrobiotic acid (7-oxo-DHA) was identified.

300 According to Ren et al. (2015), the hydroxyl group is formed first through the attack of
301 oxygen, resulting in the isomerization of the conjugated band. At the same time, the methylene is
302 converted to a hydroxyl intermediate by an oxygen atom.

303 In order to compare the different rosin samples, the surfaces of the different peaks, normalized
304 to 100, are calculated. With this technique, the concentration variation can be compared. The surfaces
305 are presented in table 1.

306 *Table 1: Comparison of abietane-based acids and derivatives contents in rosins according to their*
307 *heat treatment. The standard deviation is calculated over 15 samples.*

308 An apparition of dehydrogenated forms of abietane-based acids is noticed in heat-treated
309 rosins. For the DHA, this dehydrogenation leads to an aromatisation, and for the 7-oxo-DHA, it occurs
310 along with an oxidation. This has not been observed before, previous results presented by Cabaret et
311 al. (2018) only show heat-treated rosins, and the results presented by Kersten et al. (2006) show the
312 presence of DHA in [reference](#) rosin. Resin samples tested in [Kersten et al. paper](#) were obtained after
313 industrial distillation process [during](#) purification of Tall oil, which is a waste obtained from Kraft pulp.
314 This process might have been done at higher temperature than Biolandes process, and could be at the
315 origin of isomerization and degradation.

316 The presence of levopimaric acid was not observed. [Classical](#) acid portion of commercial pine
317 oleoresin contains from 23 to 40 % levopimaric acid, which is completely isomerized to other resin
318 acids during distillation (Loeblich et al., 1955). According to our study, this is probably due to the
319 isomerization of levopimaric acid into palustric, abietic and neoabietic acids during the distillation
320 process. The chromatogram obtained from levopimaric acid after heating at 155 °C for 3 hours by
321 Loeblich et al. (1955) is presented in Fig. 10.

322 *Figure 10: Chromatogram of levopimaric acid, heated at 155 °C for 3 hours, obtained by Loeblich,*
323 *(1) palustric acid; (2) abietic acid; (3) neoabietic acid*

324 The chromatogram closely [resembles](#) the one obtained in this study if we compare [the](#)
325 [reference](#) and heat-treated rosins, with the same elution order. The palustric, abietic and neoabietic
326 acids obtained here are therefore derived from the isomerization of levopimaric acid, which occurs
327 during the hydrodistillation of the resin.

328 Cabaret et al., (2019) showed the presence of levopimaric, abietic and neoabietic acids in rosin
329 obtained directly by heating the maritime pine resin at 60 °C and 90 °C, rosin that has not been
330 hydrodistilled. In this study, the proportion of neoabietic acid is greater than the proportion of abietic
331 and levopimaric acids, while palustric acid does not appear. We used [a](#) similar HPLC analysis

332 program as was used by Cabaret et al. (2019). We were therefore able to compare the results. The
333 hypothetical order of isomerization may be the following: levopimaric acid isomerises to abietic acid
334 and neoabietic acid. At higher temperatures, that of hydrodistillation, levopimaric acid also isomerises
335 to palustric acid, which, with neoabietic acid, isomerise in abietic acid, resulting in the disappearance
336 of levopimaric acid and a higher proportion of abietic acid. The isomerisation pathways could be
337 checked by comparing the spectra of pure palustric, abietic and neoabietic acids with the spectra of
338 pure levopimaric acid heated at different temperatures.

339 These results also show that the Biogemme® hydrodistillation process, at low pressure and low
340 temperature, could have been done at a temperature higher than 90 °C.

341 The appearance of dehydrogenated and oxidized compounds of abietane-based acids, observed
342 in thermally treated rosins, is associated with a decrease of abietane-based acids. Heat treatment can
343 therefore cause dehydrogenation of the palustric, neoabietic and abietic acids in DHA and DHABA,
344 lowering their proportions. Dehydrogenic acids also undergo oxidation, leading to the 7-oxo-DHA
345 formation.

346 This analysis confirms the chemical transformation of rosin, which can affect phase transitions
347 at higher temperatures observed in TMA and DSC.

348 3.3 Varnish properties

349 3.3.1 Physical properties

350 The film thickness, measured in the reference and the heat-treated rosins, is presented in table
351 2. The test is performed to ensure the homogeneity of the batch. According to the student test, the raw
352 rosin is different from the heat-treated ones. It can be explained by the small standard deviation of this
353 sample.

354 *Table 2 : Varnish colours according to the rosin heat treatment expressed using the CIELAB colour*
355 *space. Three measurements were made on each of the three panels. The standard deviation is*
356 *calculated over 9 measurements.*

357 *These* results show that the film thickness is homogeneous with brush application.

358 The colours' measurements are presented in Fig. 11. No relevant difference is noticed, which
359 is confirmed by the student test.

360 *Figure 11: Varnish colours according to the rosin heat treatment expressed using the CIELAB colour*
361 *space. Three measurements were made on each of the three panels. The standard deviation is*
362 *calculated over 9 measurements.*

363 Only one coordinate is different: the b* value is different for the varnish formulated if
364 compared with *the reference*. The varnishes formulated with the heat-treated rosins are more yellow,
365 which might be due to the rosin oxidation with heat treatment (observed with HPLC). *Also, rosin is*
366 *known for having a yellowing effect (Domene-López et al., 2018).*

367 The brightness is presented in Fig. 12. It seems to decrease with the heat treatment, but,
368 according to the student test, only the raw rosin is significantly different from the other ones. It means
369 that in order to obtain a less brightening coating, rosin has to undergo heat treatment.

370 *Figure 12: Brightness variation at 60 ° for varnishes according to the rosin heat treatment. Three*
371 *measurements were made on each of the three panels. The standard deviation is calculated over 9*
372 *measurements.*

373 3.3.2. Mechanical properties

374 The adhesion performances are presented in Fig. 13. All varnishes present good adherence on
375 wood, with no grade above 2. According to the student test, there is no significant difference between
376 the samples.

377 *Figure 13: Comparison of varnish adhesion on wood for varnishes according to the rosin heat*
378 *treatment. Three measurements were made on each of the three panels. The standard deviation is*
379 *calculated over 9 measurements.*

380 The solvent resistance, according to the standard, is evaluated with the apparition of blistering.
381 No blistering is noticed on the film, but a loss of brightness and a deepening is observed. The results
382 are presented in table 3.

383 *Table 3: Comparison of brightness and colour loss after a solvent test for varnishes according to the*
384 *rosin heat treatment. Three measurements were made on each of the three panels. The standard*
385 *deviation is calculated over 9 measurements.*

386 A noticeable loss of brightness and a change of colour are observed for every varnishes. For
387 all the samples, the varnish is deeper, less green and less yellow. The difference in L* and a* is more
388 important for the heat-treated rosin, while the difference in b* and brightness is similar for all rosins.
389 **These** results show a lower solvent resistance for the heat-treated rosin, which may be due to a higher
390 solvent sensibility of the dehydrogenated and oxidized compounds of abietane-based acids.

391 3.4 PCA analysis

392 From thermal analysis, chemical analysis and varnish properties, and using the R Studio
393 software, a PCA was performed. The aim was to investigate some similarities and differences between
394 the samples, according to the rosin heat treatment, and the influence of the variables on each other.

395 PC1 and PC2 together represent 78 % of the total variability. The PC1 is mainly representative
396 (64,6 %), and is based on the chemical differences in abietane-based acids and derivatives, the thermal
397 properties and some varnish properties (brightness, brightness loss, L* loss and b*). The PC2 is
398 representative of some colour characteristics (L*, a*). The representation of PC1 vs. PC2 **shows** the
399 variable position and their corresponding correlations. In fact, the variable position from one to
400 another can be correlated: their opposition means that these variables are inversely proportional.

401 The PCA biplot is presented in Fig. 14. The three representative values of the groups (non-
402 treated rosin, 180 °C, 200 °C and 250 °C treated rosin) are represented in the same graphic as the
403 variables.

404 *Figure 14: Biplot: Projection of variables and samples onto the first two PCs. (1, 2, 3) for reference*
405 *rosin; (4, 5, 6), (7,8,9) and (10, 11, 12), respectively for 180 °C, 200 °C and 250 °C heat-treated rosin*

406 The PC1 allows a good separation of the samples according to their heat treatment, with 64,6
407 % of the total variance: G1 (represented by the yellow point) is the raw rosin group, G2 (represented
408 by the green point) is the 180 °C heat-treated rosin, G3 (represented by the blue point) is the 200 °C
409 heat-treated rosin and G4 (represented by the deep blue point) is the 250 °C heat-treated rosin. This
410 spatial distribution demonstrates the influence of the heat treatment on both the rosin properties and
411 the varnish properties.

412 The first group (G1) is characterized by the presence of abietane-based acids without
413 degradations, the varnish brightness and the high amount of turpentine left in the rosin. It is also
414 characterized by a low softening point and a low glass transition temperature, along with a small
415 amount of abietane-based acids with degradations. G2 is characterized by the same variables as G1,
416 but less marked than G1. The characteristic variables of G3 are the softening point, the Tg and the
417 presence of dehydrogenated and oxidized compounds of abietane-based acids. G4 has the same
418 characteristic, but stronger than G3.

419 The PCA also shows the influence of the variables on each other. It is clear on the PC1 that the
420 turpentine amount seems to have an impact on the glass transition and the softening point; when the
421 amount of turpentine increases, the temperatures decrease. This allows a visual observation of the
422 results obtained with the thermal analysis of the rosin. The dehydrogenated and oxidized form of
423 abietic-based acid seems to have an influence on the brightness and the solvent resistance (brightness
424 loss). Their presence causes a lower brightness, and a more important loss of brightness in the
425 presence of solvent, which also allows a visual observation of the varnishes properties' results.

426 4. Conclusion

427 The heat treatment has an impact on thermal properties, as the softening point and a phase
428 transition temperature, which can be compared to the glass transition temperature, increase with the
429 temperature. The turpentine amount, as expected, is lower when rosins are heated. The heat treatment
430 also causes the apparition of dehydrogenated and oxidised forms of abietane-based acid. For the first
431 time, we have shown the presence of abietane-based acid only, without their degraded form in non-
432 treated rosin, probably due to the innovative Biogemme® distillation process at low temperature.
433 However, the chemical composition changes could be further confirmed with elementary analysis for
434 the C, O and H content.

435 This study shows the relevance of the rosin heat treatment for varnish formulation. The
436 varnish films are less bright when formulated with heat-treated rosin. It can be interesting for the
437 customer demand, which can change from a very bright to a natural aspect coating. However, the
438 solvent resistance seems to decrease with the heat treatment, probably due to a higher sensibility of the
439 dehydrogenated and oxidised forms of abietane-based acid to the sodium hydroxide solution.

440 The PCA allows us to have a spatial repartition of the samples groups, according to their
441 results. In addition, some variables affect each other. Thanks to the PCA, the impact of the heat
442 treatment on the thermal and the varnish properties, through the chemical composition change, can be
443 observed visually.

444 From this study, a better understanding of the formulation aspect of bio-based varnishes with
445 rosin can be expected.

446 Acknowledgements

447 We gratefully acknowledge the financial support from the Nouvelle Aquitaine region and the
448 Landes departmental council. This work was also funded by ANR-10-EQPX-16 XYLOFOREST
449 (Mont-de-Marsan). We gratefully acknowledge the support from our partner Holiste. We also
450 acknowledge Roxane Le Corre for the English editing.

451 Bibliography

452 Artaki, I., Ray, U., Gordon, H.M., Gervasio, M.S., 1992. Thermal degradation of rosin during high
453 temperature solder reflow. *Thermochimica acta* 198, 7–20.

454 Baldwin, D., Loeblich, V., Lawrence, R., 1958. Acidic Composition of Oleoresins and Rosins. *Ind.*
455 *Eng. Chem. Chem. Eng. Data Series* 3, 342–346. <https://doi.org/10.1021/i460004a036>

456 Berg, J.D.J. van den, 2002. Analytical chemical studies on traditional linseed oil paints, *MolArt.*
457 *FOM-Institute AMOLF*.

458 Blanche, C.A., Lorio, P.L., Sommers, R.A., Hodges, J.D., Nebeker, T.E., 1992. Seasonal cambial
459 growth and development of loblolly pine: Xylem formation, inner bark chemistry, resin ducts, and
460 resin flow. *Forest Ecology and Management* 49, 151–165. <https://doi.org/10.1016/0378->
461 [1127\(92\)90167-8](https://doi.org/10.1016/0378-1127(92)90167-8)

462 Byrdwell, W.C., Neff, W.E., 1999. Non-volatile products of triolein produced at frying temperatures
463 characterized using liquid chromatography with online mass spectrometric detection. *Journal of*
464 *Chromatography A* 852, 417–432. [https://doi.org/10.1016/S0021-9673\(99\)00529-4](https://doi.org/10.1016/S0021-9673(99)00529-4)

465 Cabaret, T., Boulicaud, B., Chatet, E., Charrier, B., 2018. Study of rosin softening point through
466 thermal treatment for a better understanding of maritime pine exudation. *European Journal of Wood*
467 *and Wood Products* 76, 1453–1459. <https://doi.org/10.1007/s00107-018-1339-3>

468 Cabaret, T., Gardere, Y., Frances, M., Leroyer, L., Charrier, B., 2019. Measuring interactions between
469 rosin and turpentine during the drying process for a better understanding of exudation in maritime pine
470 wood used as outdoor siding. *Industrial Crops and Products* 130, 325–331.
471 <https://doi.org/10.1016/j.indcrop.2018.12.080>

472 Carson, P., Mumford, C., 2002. 6 - Flammable chemicals, in: Carson, P., Mumford, C. (Eds.),
473 *Hazardous Chemicals Handbook (Second Edition)*. Butterworth-Heinemann, Oxford, pp. 178–227.
474 <https://doi.org/10.1016/B978-075064888-2/50007-4>

475 Chen, G.-F., 1992. Developments in the field of rosin chemistry and its implications in coatings.
476 *Progress in Organic Coatings* 20, 139–167. [https://doi.org/10.1016/0033-0655\(92\)80002-E](https://doi.org/10.1016/0033-0655(92)80002-E)

477 Cheniclet, C., 1987. Effects of Wounding and Fungus Inoculation on Terpene Producing Systems of
478 Maritime Pine. *J Exp Bot* 38, 1557–1572. <https://doi.org/10.1093/jxb/38.9.1557>

479 Coppen, J.J.W., Hone, G.A., 1995. Gum naval stores, turpentine and rosin from pine resin. Food and
480 Agriculture Organization of the United Nations 1–62.

481 de Viguerie, L., Payard, P.A., Portero, E., Walter, Ph., Cotte, M., 2016. The drying of linseed oil
482 investigated by Fourier transform infrared spectroscopy: Historical recipes and influence of lead
483 compounds. *Progress in Organic Coatings* 93, 46–60. <https://doi.org/10.1016/j.porgcoat.2015.12.010>

484 Domene-López, D., M. M. Guillén, I. Martín-Gullón, J. C. García-Quesada, et M. G. Montalbán.
485 2018. « Study of the Behavior of Biodegradable Starch/Polyvinyl Alcohol/Rosin Blends ». *Carbohydrate Polymers* 202 (décembre): 299-305. <https://doi.org/10.1016/j.carbpol.2018.08.137>.

487 Echard, J.-P., Bertrand, L., von Bohlen, A., Le Hô, A.-S., Paris, C., Bellot-Gurlet, L., Soulier, B.,
488 Lattuati-Derieux, A., Thao, S., Robinet, L., Lavédrine, B., Vaiedelich, S., 2010. The Nature of the
489 Extraordinary Finish of Stradivari's Instruments. *Angewandte Chemie International Edition* 49, 197–
490 201. <https://doi.org/10.1002/anie.200905131>

491 Echard, J.P., Malecki, V., 2014. Oil-Pinaceae resin varnish recipes in 15th-18th-century written
492 sources. pp. 131–132.

493 Franceschi, V.R., Krokene, P., Christiansen, E., Krekling, T., 2005. Anatomical and chemical defenses
494 of conifer bark against bark beetles and other pests - Franceschi - 2005 - *New Phytologist* - Wiley
495 Online Library. *New Phytol* 367, 353–376.

496 Gaillard, Y., Mija, A., Burr, A., Darque-Ceretti, E., Felder, E., Sbirrazzuoli, N., 2011. Green material
497 composites from renewable resources: Polymorphic transitions and phase diagram of beeswax/rosin
498 resin. *Thermochimica Acta* 521, 90–97. <https://doi.org/10.1016/j.tca.2011.04.010>

499 Gilles, N., 2019. A method for cooking oil varnish. *The Strad* 130, 72–75.

500 Hawkins, J.E., Armstrong, G.T., 1954. Physical and Thermodynamic Properties of Terpenes.1 III. The
501 Vapor Pressures of α -Pinene and β -Pinene2. J. Am. Chem. Soc. 76, 3756–3758.
502 <https://doi.org/10.1021/ja01643a051>

503 Hawley, L.F., Palmer, R.C., 1912. Distillation of Resinous Wood by Saturated Steam. J. Ind. Eng.
504 Chem. 4, 789–798. <https://doi.org/10.1021/ie50047a003>

505 Invernizzi, C., Daveri, A., Rovetta, T., Vagnini, M., Licchelli, M., Cacciatori, F., Malagodi, M., 2016.
506 A multi-analytical non-invasive approach to violin materials: The case of Antonio Stradivari “Hellier”
507 (1679). Microchemical Journal 124, 743–750. <https://doi.org/10.1016/j.microc.2015.10.016>

508 Joye, N.M., Lawrence, R.V., 1967. Resin acid composition of pine oleoresins. J. Chem. Eng. Data 12,
509 279–282. <https://doi.org/10.1021/je60033a034>

510 Kanerva, M., Puolakka, A., Takala, T.M., Elert, A.M., Mylläri, V., Jönkkäri, I., Sarlin, E., Seitsonen,
511 J., Ruokolainen, J., Saris, P., Vuorinen, J., 2019. Antibacterial polymer fibres by rosin compounding
512 and melt-spinning. Materials Today Communications 100527.
513 <https://doi.org/10.1016/j.mtcomm.2019.05.003>

514 Kassambara, A., 2017. Practical Guide To Principal Component Methods in R: PCA, M(CA), FAMD,
515 MFA, HCPC, factoextra. STHDA.

516 Krokene, P., 2015. Conifer Defense and Resistance to Bark Beetles, in: Bark Beetles: Biology and
517 Ecology of Native and Invasive Species. Hofstetter RW, Vega FE, pp. 177–207.

518 Lê, S., Josse, J., Husson, F., 2008. FactoMineR: An R Package for Multivariate Analysis. Journal of
519 Statistical Software 25, 1–18. <https://doi.org/10.18637/jss.v025.i01>

520 Loeblich, V.M., Baldwin, D.E., O’Connor, R.T., Lawrence, R.V., 1955. Thermal Isomerization of
521 Levopimaric Acid. J. Am. Chem. Soc. 77, 6311–6313. <https://doi.org/10.1021/ja01628a071>

522 Moreira, X., Sampedro, L., Zas, R., 2009. Defensive responses of Pinus pinaster seedlings to
523 exogenous application of methyl jasmonate: Concentration effect and systemic response.
524 Environmental and Experimental Botany 67, 94–100. <https://doi.org/10.1016/j.envexpbot.2009.05.015>

525 Narayanan, M., Loganathan, S., Valapa, R.B., Thomas, S., Varghese, T.O., 2017. UV protective
526 poly(lactic acid)/rosin films for sustainable packaging. *International Journal of Biological*
527 *Macromolecules* 99, 37–45. <https://doi.org/10.1016/j.ijbiomac.2017.01.152>

528 Pastorova, I., van der Berg, K.J., Boon, J.J., Verhoeven, J.W., 1997. Analysis of oxidised diterpenoid
529 acids using thermally assisted methylation with TMAH. *Journal of Analytical and Applied Pyrolysis*
530 43, 41–57. [https://doi.org/10.1016/S0165-2370\(97\)00058-2](https://doi.org/10.1016/S0165-2370(97)00058-2)

531 Pinto, I., Knapic, S., Pereira, H., Usenius, A., 2005. Simulated and realised industrial yields in sawing
532 of maritime pine (*Pinus pinaster* Ait.). *Holz als Roh- und Werkstoff* 64, 30–36.
533 <https://doi.org/10.1007/s00107-005-0042-3>

534 Ren, Fan, Yan-Fei Zheng, Xiong-Min Liu, Xin-Yin Yue, Li Ma, Wei-Guang Li, Fang Lai, Jia-Ling
535 Liu, et Wen-Long Guan. 2015. « An investigation of the oxidation mechanism of abietic acid using
536 two-dimensional infrared correlation spectroscopy ». *Journal of Molecular Structure* 1084 (mars):
537 236-43. <https://doi.org/10.1016/j.molstruc.2014.12.055>.

538 Riesco Muñoz, G., Santaclara Estévez, Ó., Álvarez González, J.G., Merlo, E., 2014. Influence of
539 provenance, silvicultural regime and tree shape on the quality of maritime pine (*Pinus pinaster*) timber.
540 *European Journal of Forest Research* 133. <https://doi.org/10.1007/s10342-014-0790-x>

541 Rodríguez-García, A., López, R., Martín, J.A., Pinillos, F., Gil, L., 2014. Resin yield in *Pinus pinaster*
542 is related to tree dendrometry, stand density and tapping-induced systemic changes in xylem anatomy.
543 *Forest Ecology and Management* 313, 47–54. <https://doi.org/10.1016/j.foreco.2013.10.038>

544 Rodríguez-García, A., Martín, J.A., López, R., Sanz, A., Gil, L., 2016. Effect of four tapping methods
545 on anatomical traits and resin yield in Maritime pine (*Pinus pinaster* Ait.). *Industrial Crops and*
546 *Products* 86, 143–154. <https://doi.org/10.1016/j.indcrop.2016.03.033>

547 Rosa, R., Soares, P., Tomé, M., 2018. Evaluating the Economic Potential of Uneven-aged Maritime
548 Pine Forests. *Ecological Economics* 143, 210–217. <https://doi.org/10.1016/j.ecolecon.2017.07.009>

549 Scalarone, D., Lazzari, M., Chiantore, O., 2002. Ageing behaviour and pyrolytic characterisation of
550 diterpenic resins used as art materials: colophony and Venice turpentine. *Journal of Analytical and*
551 *Applied Pyrolysis* 64, 345–361. [https://doi.org/10.1016/S0165-2370\(02\)00046-3](https://doi.org/10.1016/S0165-2370(02)00046-3)

552 Schilling, Michael R. 1989. « The glass transition of materials used in conservation ». *Studies in*
553 *Conservation* 34 (3): 110-16. <https://doi.org/10.1179/sic.1989.34.3.110>.

554 Soliño, M., Yu, T., Alía, R., Auñón, F., Bravo-Oviedo, A., Chambel, M.R., de Miguel, J., del Río, M.,
555 Justes, A., Martínez-Jauregui, M., Montero, G., Mutke, S., Ruiz-Peinado, R., García del Barrio, J.M.,
556 2018. Resin-tapped pine forests in Spain: Ecological diversity and economic valuation. *Science of The*
557 *Total Environment* 625, 1146–1155. <https://doi.org/10.1016/j.scitotenv.2018.01.027>

558 Tirat, S., Degano, I., Echard, J.-P., Lattuati-Derieux, A., Lluveras-Tenorio, A., Marie, A., Serfaty, S.,
559 Le Huerou, J.-Y., 2016. Historical linseed oil/colophony varnishes formulations: Study of their
560 molecular composition with micro-chemical chromatographic techniques. *Microchemical Journal* 126,
561 200–213. <https://doi.org/10.1016/j.microc.2015.11.045>

562 Tirat, S., Echard, J.-P., Lattuati-Derieux, A., Le Huerou, J.-Y., Serfaty, S., 2017. Reconstructing
563 historical recipes of linseed oil/colophony varnishes: Influence of preparation processes on application
564 properties. *Journal of Cultural Heritage* 27, S34–S43. <https://doi.org/10.1016/j.culher.2017.08.001>

565 Wang, J., Lu, C., Liu, Y., Wang, C., Chu, F., 2018. Preparation and characterization of natural rosin
566 stabilized nanoparticles via miniemulsion polymerization and their pressure-sensitive adhesive
567 applications. *Industrial Crops and Products* 124, 244–253.
568 <https://doi.org/10.1016/j.indcrop.2018.07.079>

569 Wold, S., Esbensen, K., Geladi, P., 1987. Principal component analysis. *Chemometrics and Intelligent*
570 *Laboratory Systems, Proceedings of the Multivariate Statistical Workshop for Geologists and*
571 *Geochemists* 2, 37–52. [https://doi.org/10.1016/0169-7439\(87\)80084-9](https://doi.org/10.1016/0169-7439(87)80084-9)

572 Wu, H., Hu, Z., 1997. Comparative anatomy of resin ducts of the Pinaceae. *Trees* 11 132–143.

573

Table 1: Comparison of abietane based acids and derivatives contents in rosins according to their heat treatment. The standard deviation is calculated over 15 samples.

#	Molecule	Absorption max (nm)	Peak area ratio for Raw rosin	Peak area ration for 180 °C rosin	Peak area ration for 200 °C rosin	Peak area ration for 250 °C rosin
(1)	7-oxo-DHA	255.6	0	1.6±0.4	2.0±1.1	6.5±4.6
(2)	DHABA	243.5	0	0.8±0.1	1.1±0.4	1.6±0.6
(3)	DHA	225.3/252/268	0	3.8±0.4	4.5±1.7	7.0±1.6
(4)	Palustric	268	11.4±1.8	9.9±1.8	9.5±2.0	9.0±2.5
(5)	Abietic	240.8	84.3±1.6	85.8±3.9	81.5±2.7	73.1±7.6
(6)	Neobietic	252	4.1±2.3	5.0±0.8	3.4±0.8	1.1±1.4

Table 2 : Varnish colours according to the rosin heat treatment expressed using the CIELAB colour space. Three measurements were made on each three panels. The standard deviation is calculated over 9 measurements.

Value	Raw	180 °C	200 °C	250 °C
L*	54.30±3.76	54.33±1.86	55.92±0.91	54.79±2.43
a*	17.26±2.85	16.78±1.04	16.07±0.71	16.81±1.17
b*	52.55±1.34	48.09±1.90	47.56±2.98	47.63±3.19

Table 3: Comparison of brightness and colour loss after a solvent test for varnishes according to the rosin heat treatment. Three measurements were made on each three panels. The standard deviation is calculated over 9 measurements.

Value	Raw	180 °C	200 °C	250 °C
-------	-----	--------	--------	--------

L*	-7.3±2.4 %	-13.0±4.0 %	-15.1±0.6 %	-19.2±1.7 %
a*	+5.4±9.2 %	+9.8±4.3 %	+32.1±5.5 %	+15.0±5.9 %
b*	-26.9±1.1 %	-21.3±3.6 %	-19.3±2.1 %	-24.9±2.5 %
Brightness	-89.2±5.3 %	-92.2±7.2 %	-95.7±8.1 %	-96.2±16.1 %

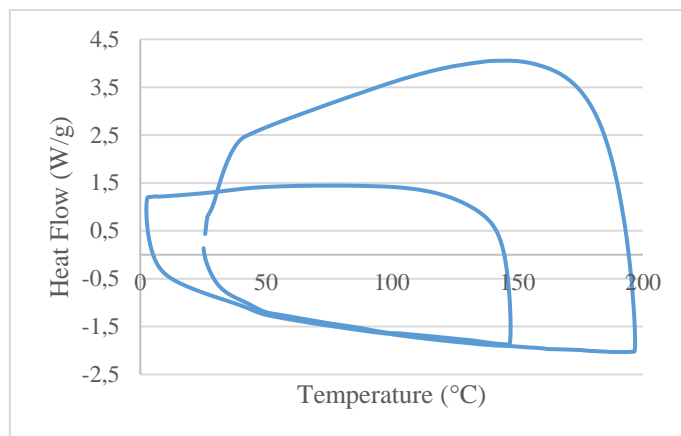


Figure 1 : DSC thermogram of reference rosin in a range from 5 °C to 200 °C

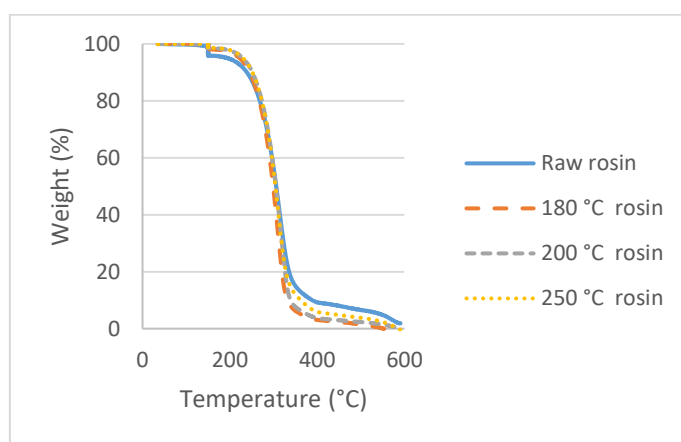


Figure 2 : TGA thermograms of rosin according to their heat treatment

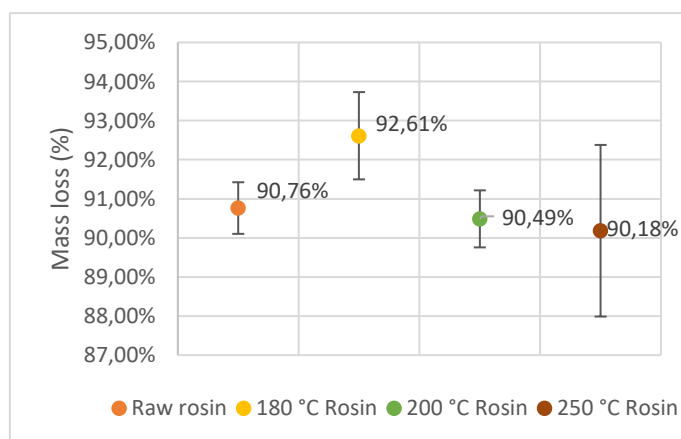


Figure 3: Comparison of the final mass loss of rosin according to their heat treatment. The standard deviation is calculated over 3 samples.

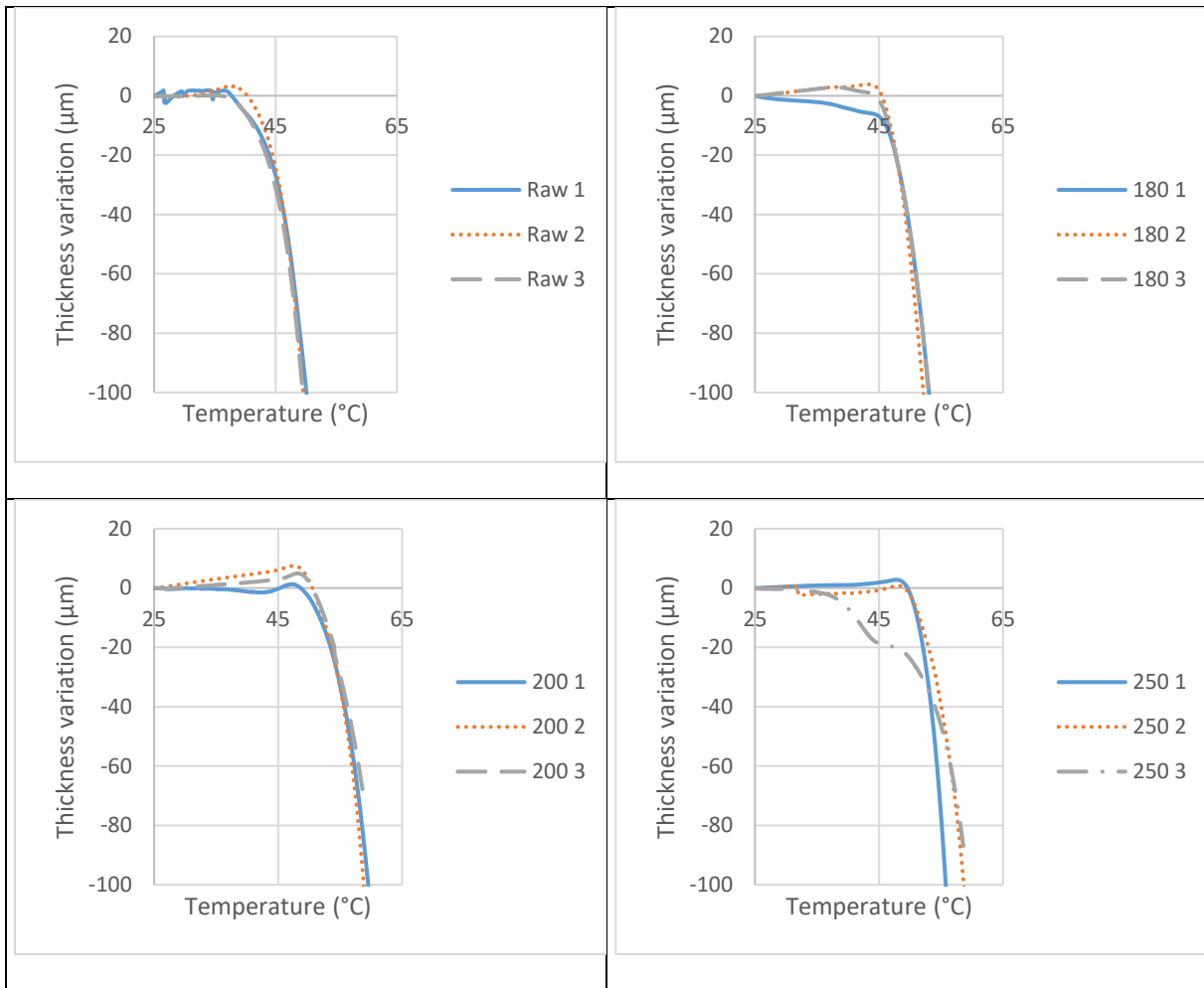


Figure 4: Thickness variation against temperature for rosins according to their heat treatment

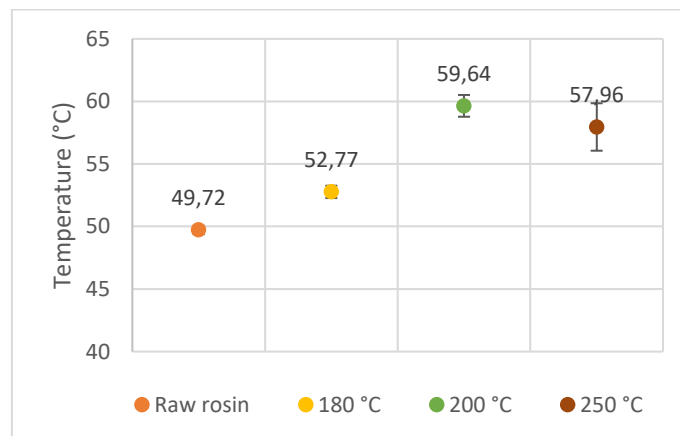


Figure 5: Comparison of the rosin softening point temperature according to their heat treatment. The standard deviation is calculated over 3 samples.

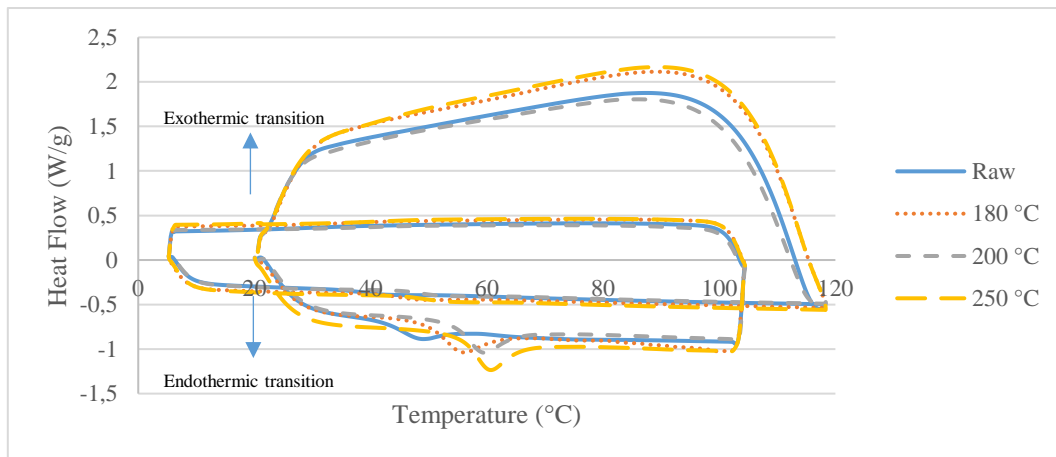


Figure 6 : DSC curves obtained for *rosins* according to their heat treatment

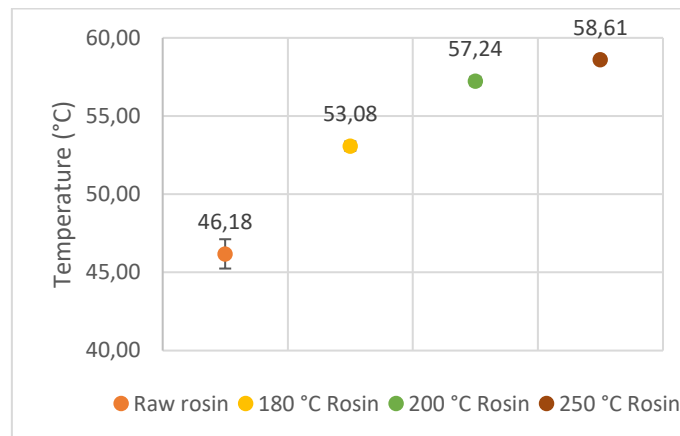


Figure 7: Comparison of the rosin *glass* transition temperature according to their heat treatment. The standard deviation is calculated over 3 samples.

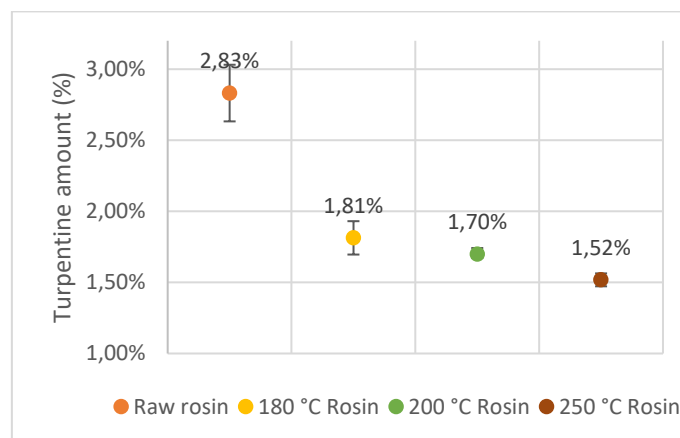


Figure 8: Comparison of the turpentine amount in rosin according to their heat treatment. The standard deviation is calculated over 3 samples.

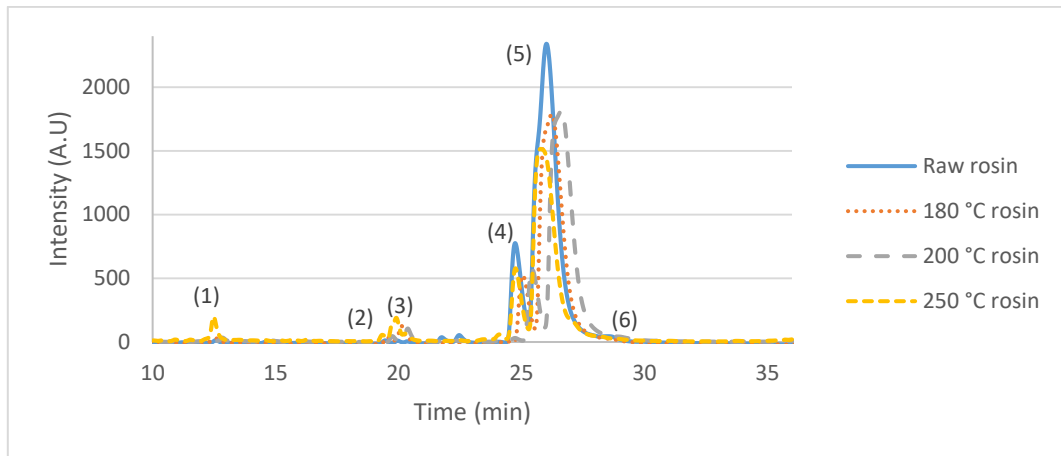


Figure 9: HPLC chromatograms at 254 nm wavelength absorption of rosins according to their heat treatment. (1) 7-oxo-dehydroabietic acid (7-oxo-DHA), (2) Abietane-based dehydroabietic acid (DHABA), (3) Dehydroabietic acid (DHA), (4) Palustric acid, (5) Abietic acid, (6) Neoabietic acid

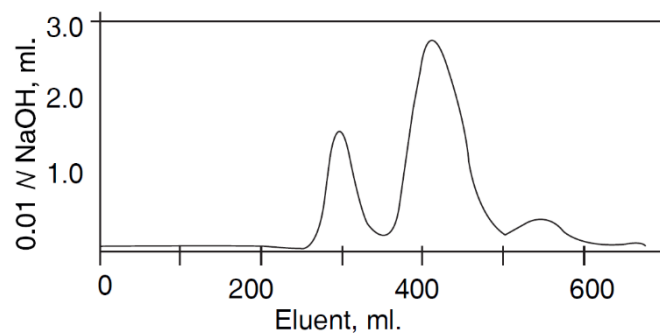


Figure 10: Chromatogram of levopimaric acid, heated at 155 °C during 3 hours, obtains by Loeblich, (1) palustric acid; (2) abietic acid; (3) neoabietic acid

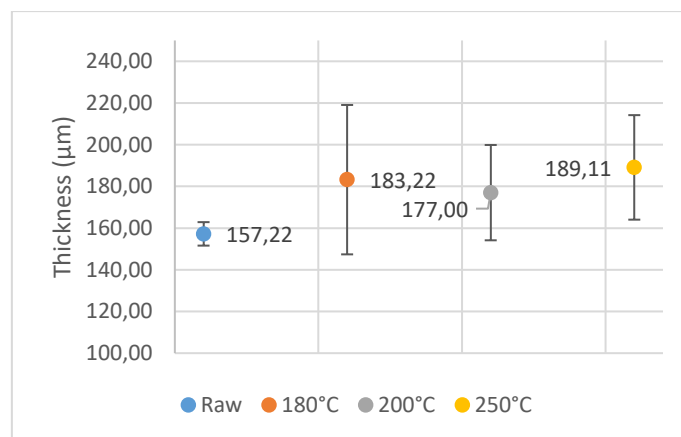


Figure 11: Thickness variation for varnishes according to the rosin heat treatment. Three measurements were made on each three panels. The standard deviation is calculated over 9 measurements.

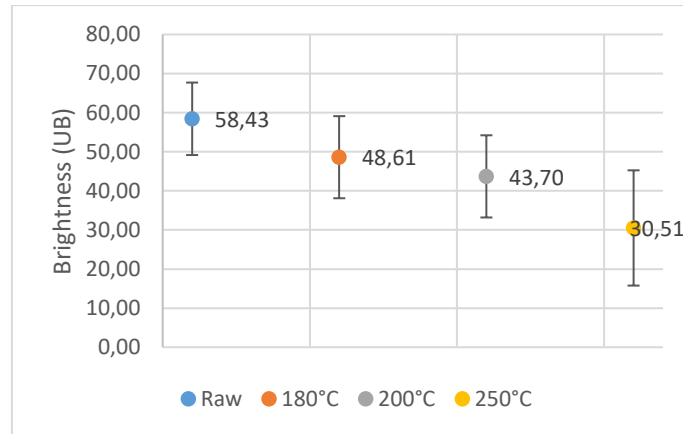


Figure 12: Brightness variation at 60 ° for varnishes according to the rosin heat treatment. Three measurements were made on each three panels. The standard deviation is calculated over 9 measurements.

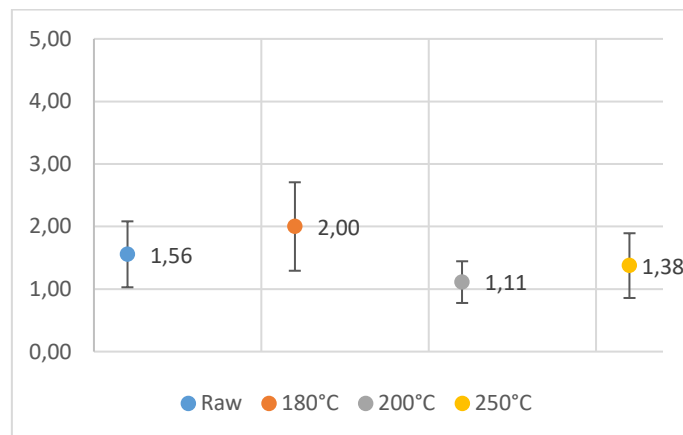


Figure 13: Comparison of varnish adhesion on wood for varnishes according to the rosin heat treatment. Three measurements were made on each three panels. The standard deviation is calculated over 9 measurements.

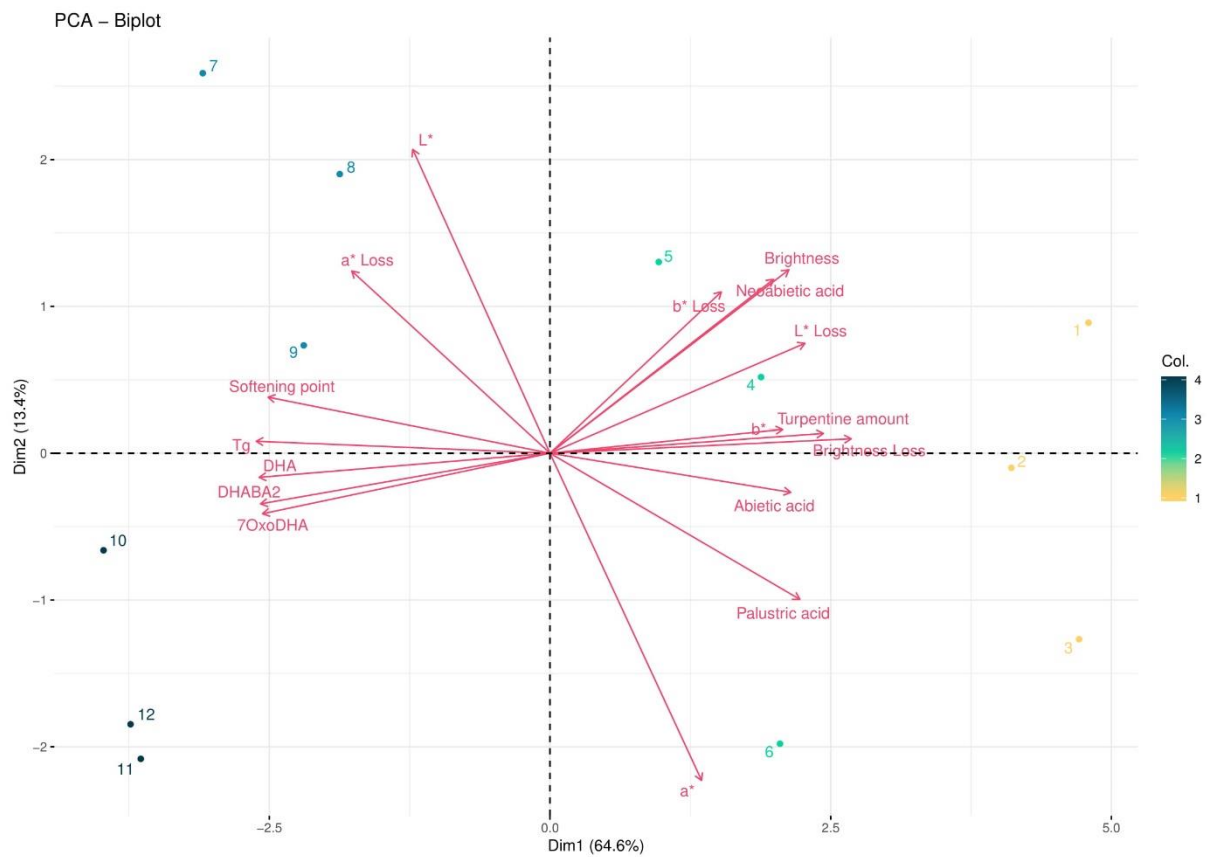


Figure 14: Biplot : Projection of variables and samples onto the first two PCs. (1, 2, 3) for *reference* rosin; (4, 5, 6), (7,8,9) and (10, 11, 12), respectively for 180 °C, 200 °C and 250 °C heat-treated rosin

